Thermal Transport Properties of Bi_2O_2Se-Ag_2Se Hybrid Structures

M. Umer Farooq[a,*], Sumayya[b], M. Umer Iqbal[b], Ishrat Asghar[a], Mujtaba Ikram[c], Sajid Butt[d]

[a]*Department of Physics, University of Education (Lahore), Faisalabad Campus.*
[b]*Department of Materials Science and Engineering, Institute of Space Technology, Islamabad 44000, Pakistan*
[c]*Institute of chemical engineering and technology (ICET), University of Punjab, Lahore Pakistan*
[d]*Department of Space Science, Institute of Space Technology, Islamabad 44000, Pakistan*
Received: August 31 2021, Accepted: January 26, 2022 Published: November 30, 2021

Abstract

The series of Bi_2O_2Se-Ag_2Se composites were synthesized by two step solid state reaction followed by Spark plasma sintering. To optimize their thermal transport properties, different weight percent (wt. %) of silver i-e, 10%, 15% and 20%, was added. The room temperature X-ray diffraction (XRD) and high temperature XRD was used to investigate the crystalline phases, whereas the morphological study was conducted through FESEM. The thermal transport properties were evaluated from 323 K to 773 K, to study the effect of silver addition on thermal conductivity of all the composite samples. The reduced thermal conductivity of the composite with decreasing Ag contents is might be attributed to increase of the Ag_2Se and Bi_2O_3 nano-inclusions in Bi_2O_2Se multi-phase-system that increased the phonon scattering regions and reduced the overall thermal conductivity significantly, up to 54 % for BA15SO as compared to that of BA20CO at 473 K.

Introduction

To fulfill the world's energy gap, researchers are in continuous search of alternative energy sources and thermoelectric materials (TEMs) are potential candidate [1]. The TEMs have the distinct ability in inter-conversion of heat and electricity [2-5]. The inter-conversion efficiency of TEMs is calculated by a dimensionless figure of merit (ZT). The *ZT* depends upon three interlinked variables i-e, electrical conductivity (σ), Seebeck coefficient (S) and total thermal conductivity (*k*). The total thermal conductivity (*k*) is the sum of electronic thermal conductivity (k_e) and lattice thermal conductivity (k_l). $k = k_e + k_l$. The expression is, ZT= $(\sigma S^2/k)T$, whereas T is absolute temperature [6-8]. Hence, according to the *ZT* expression, the efficient TEMs must exhibits high electrical conductivity, large Seebeck coefficient and low thermal conductivity. Due to inter-coupled effects of electrical and thermal conductivity, it is a difficult task to optimize the thermoelectric transport properties of TEMs [9-11]. Therefore, finding the new efficient thermoelectric materials or designing the potent strategies to resolve the interrelated electrical and thermal conductivity parameters, provide quantum leap in the field of thermoelectric research [12-14].

The n-type oxygen containing semiconductors (OCS) are considered as promising TEMs as compared to p-type oxygen containing semiconductors. This privilege is due to their stable behavior towards thermal and chemical properties. However, their moderate electrical conductivity but high thermal conductivity proved to be challenging towards the optimization of the thermoelectric transport properties. Another problem in the structure of OCS is the presence of highly electronegative oxygen atom which retards the mobility of carriers and its light weight associated with high sound speed results in high thermal conductivity [12].

Thermoelectric community is curious about bismuth based oxy-chalcogenides such as Bi_2O_2Se compound due to its enthralling layered structure. The structure is comprised of insulating layers of $[Bi_2O_2]^{2+}$ which are stacked alternatively on the conductive layers of $[Se]^{2-}$. This unique layered structure and anionic chemical bonding gives rise to intrinsic low thermal conductivity in the Bi_2O_2Se in the range of 0.7-0.8 $Wm^{-1}K^{-1}$ but high carrier mobility of ≈100 cm2 V^{-1} s^{-1} as well as large Seebeck coefficient of ≈500 μV K^{-1} [14]. These characteristics are enough to considered Bi_2O_2Se as a potential candidate for thermoelectric applications. On the other hand its carrier concentration is very limited but this property can be increased by elemental doping and as a result, its thermoelectric efficiency can be improved [13]. According to the study carried out by Cheng et al., Bi_2O_2Se have a zipper like layered structure and there is no obvious gap between the insulating and conductive layers. These layers experience strong interlayer force of attraction. This unique 2D assembly suggests many noteworthy aspects to be discovered [15].

As we have discussed earlier that elemental doping is one among many strategies that can enhance the thermoelectric efficiency of bismuth based oxy-chalcogenides. Elemental dopants like Cl, Te, Ta [16], Ge [1], Sb [17], Nb [18], S [19] and Ag [20] have been successfully doped in Bi_2O_2Se and results in improved thermoelectric properties as compared to their parent compounds.

In this work, we have synthesized a series of Bi_2O_2Se-Ag_2Se composites by varying silver concentrations by weight percent (10%, 15%, and 20% named as ((BA10SO, BA15SO and BA20SO) through two-step solid state reaction method. The correlation between the thermal transport properties and the crystalline phases was thoroughly investigated, which provided us new insight knowledge for controlling the thermal conductivity of n-type Bi_2O_2Se by incorporation of more number of scattering regions through silver addition.

Experimental

The n-type Bi_2O_2Se-Ag_2Se composite material has been synthesized by 2-step solid state reaction. A stoichiometric amount of Bi (4N), Bi_2O_3 (4N), and Se (5N) along with different weight percent (10%, 15% and 20%) of Ag(5N) powder, were mixed in a ball milling at 350 RPM for 5 hours. The mixed powders were compacted into pellets using cold press and sealed in an evacuated quartz tube. The sealed pellets were annealed in furnace first at 573K for 8 hours, which were then heated again at 873K for 24 hours in Argon environment to avoid any reaction. The annealed samples were ball milled again in a planetary ball milling at 450RPM for 5 hours. The obtained powders were compacted to bulk by Spark Plasma Sintering (SPS) under a uniaxial pressure of 50MPa for 6 minutes. A pellet of length and width $\varphi = 10mm$ was cut for thermal conductivity measurement.

The microstructures and grain morphologies were studied using field emission scanning electron microscope (FESEM). The

https://doi.org/10.24949/njes.v14i2.662

structural analysis of all the series of specimens was investigated by XRD, panalytical X'pert diffractometer with Cu-k_α radiations at various temperature ranges.

The thermal diffusivity (D) and the heat capacity (C_p) were measured by NetzschLFA 457 using Laser Flash Method along the thickness direction of square pellet. The total thermal conductivity (k) was calculated by the formula;$k = DCpd$, where, d is the mass density measured by Archimedes principle.

Results and Discussion

The crystal structure and the phases in all the Ag added Bi_2O_2Se samples were determined through their XRD patterns and compared with the standard PDF cards. In the Figure 1, these XRD patterns of all the composites samples closely indexed with the pure Bi_2O_2Se, which was simulated through the its standard card indexed as PDF#25-1463. Here, the slight peak shift (<0.1°) towards higher θ as well as the increase in the lattice parameters is observed in all Ag added samples as compare to the simulated Bi_2O_2Se pattern as shown in the Table 1, which is mainly due to the slight substitution of Ag in the crystal lattice of Bi_2O_2Se as the ionic radii of Ag is smaller than that of Bi. This peak shift increases with higher addition of Ag in the Bi_2O_2Se. Moreover, It can clearly be seen that the peaks indexed to the PDF#24-1041 (between~35 to 45:2θ) begins to appear and get dominated with the further addition of Ag in the Bi_2O_2Se. Similarly, the intense characteristic peaks of Bi_2O_2Se also broaden with the this Ag addition indexed to the PDF#75-0993 ($Bi_2O_{2.7}$). This data reveals that all the Ag added samples contain predominate phase of tetragonal Bi_2O_2Se along with Ag_2Se (β) and $Bi_2O_{2.7}$ (α) as two secondary phases and these $Bi_2O_{2.7}$ and Ag_2Se phases increased with further addition of Ag, where these secondary phases originated as a result of the reaction between the added Ag with the Bi_2O_2Se consistent with the previously reported work [20]. Figure 2 represents the XRD patterns for BA20SO at four different temperatures, where the effect of temperature on the crystal structure of BA20SO was examined. Here, the overall structure is predominately remains same throughout the temperature range, which is tetragonal Bi_2O_2Se as indexed to the PDF#25-1463.

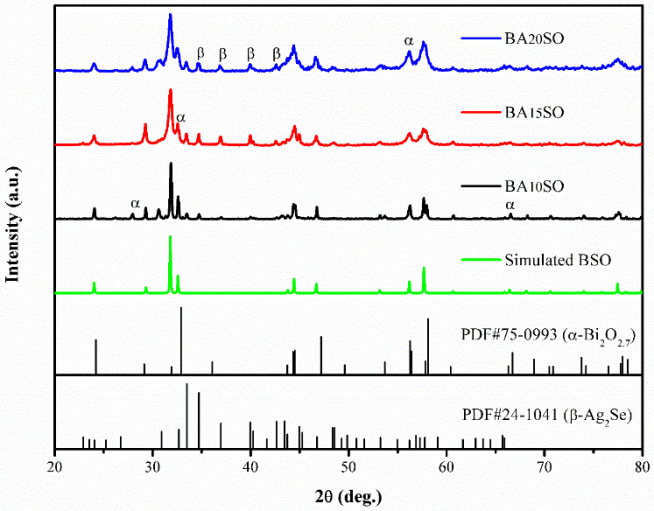

Figure 1: XRD data of Ag added Bi_2O_2Se samples

Table 1. Lattice parameters of pure and Ag added Bi_2O_2Se

Sample Name	a=b	c	α=β=γ
Simulated BSO	3.8757	12.1776	90
BA10SO	3.8796	12.1917	90
BA15SO	3.8854	12.2064	90
BA20SO	3.8888	12.2032	90

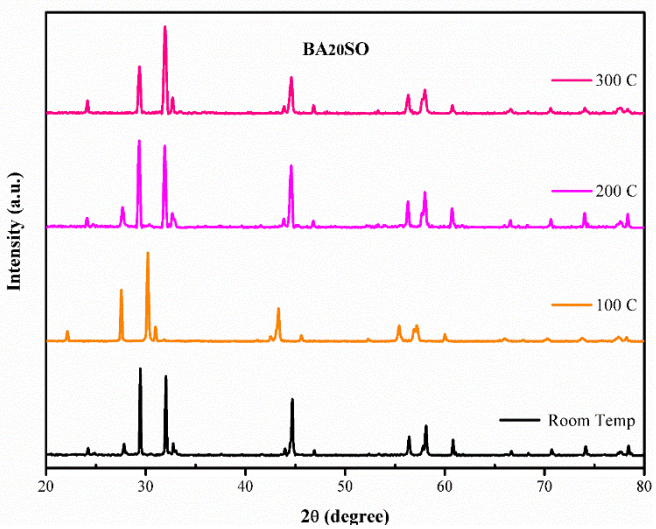

Figure 2: High temperature XRD data of BA20SO (20% Ag added Bi_2O_2Se)

However the peak shift of all the peaks to lower θ may be due to the release of lattice stresses as the temperature reached 100 C similar to the annealing process. But upon further increase of temperature to 200 C and 300 C, the peaks shifts towards higher θ may be due to the induction of thermal stresses [21].

The FESEM images of BA15SO composite specimen of the fractured surface are shown in figure 3. In figure 3a, the low magnification FESEM image of BA15SO shows a typical lamellar structure with some porosity could be seen clearly. However in Figure 3b, the composite sample clearly express the effect of silver doping in Bi_2O_2Se [20]. The microstructure of composite becomes dense due to increase in the size of grains (< 1 μm). Here, some well dispersed nano-particles can be seen into the lattice of the microsized grains which might be Ag_2Se. However, further investigation is required to confirm these nanosized particles. Thus, these nanoinclusion are responsible to create additional grain boundaries to create high energy phonons that are responsible for ultra-low lattice thermal conductivity of the multi-phased composite system.

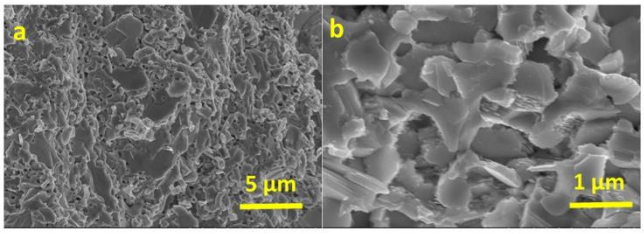

Figure 3: SEM images of (a) Bi_2O_2Se (b) Bi_2O_2Se-Ag_2Se Composite

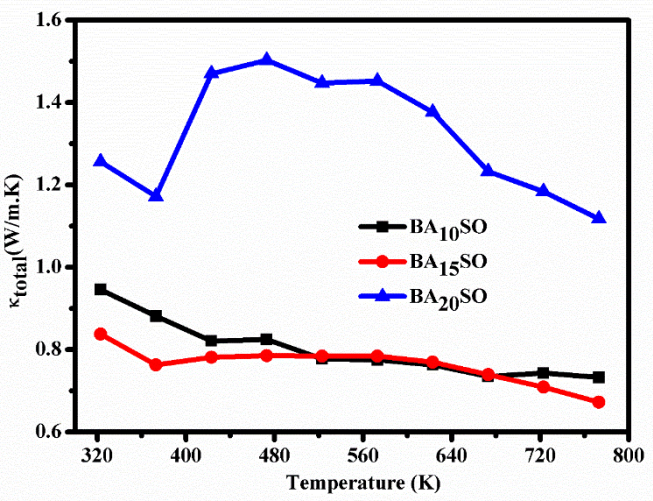

Figure 4: Temperature dependent thermal conductivity of Ag added Bi_2O_2Se

The temperature dependent thermal conductivities of all the composite samples between 323 K and 773 K are shown in figure 4. The total thermal conductivity is found to be decreased with increased temperature. A sudden change in trend has been observed clearly near 400 K in all the samples which might be due to change from one phase. The total thermal conductivity has been increased with increasing Ag content. But the sample BA15SO shows minimum total thermal conductivity of 0.67 W/mK at 773 K, which shows that a controlled addition of Ag may lead to enhance the phonon scattering regions, which may lead to reduce the lattice contribution as shown in figure 5. This possible reduction in the lattice thermal conductivity is might be due to the nano-inclusion of Ag_2Se and $Bi_2O_{2.7}$ into the matrix of Bi_2O_2Se [22], which might increase the grain boundaries and phonon scattering centers.

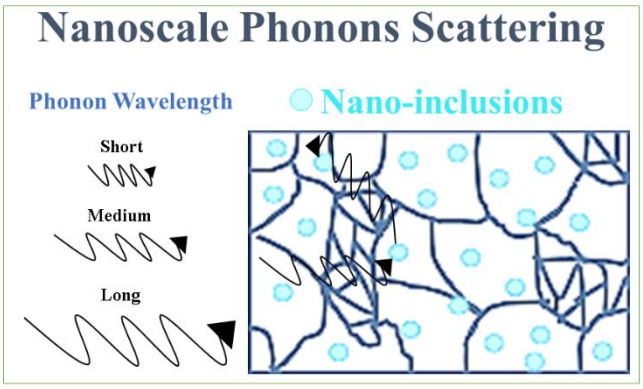

Figure 5: Phonons scattering through nano-inclusion in Ag added Bi_2O_2Se grains

This decrease might also be due to the formation of precipitates of secondary phases between the grains, which results in strong scattering of medium range phonons as previously reported [20, 23]. In BA10SO and BA15SO, the main contribution towards the reduced total thermal conductivity is the sufficiently suppressed lattice thermal conductivity, which could be attributed towards the multi-phased system combined with nano-inclusion of the secondary phase, which collectively increased the phonon scattering centers to decline the total thermal conductivity. However in BA20SO, the total thermal conductivity has shown incredible increment, especially at 473 K, where k is increased up to 54 % as compared to that of BA15SO, which might be due the presence of unreacted silver between the grains as it has been previously reported that the higher addition of silver in matrix lead to considerable enhancement of thermal conductivity [20, 24, 25].

Conclusion

The multi-phased system mainly consisted of Bi_2O_2Se-Ag_2Se composites along with minute $Bi_2O_{2.7}$ phase have been synthesized by two step process followed by spark plasma sintering. A typical lamellar structure with some porosity was found in BA15SO, where some well dispersed nanoinclusion are responsible in the scattering of medium wavelength phonons that are responsible for ultra-low lattice thermal conductivity of the multi-phased composite system in BA10SO and BA15SO. The XRD patterns also confirm the presence of minute $Bi_2O_{2.7}$ and Ag_2Se phases along with predominate Bi_2O_2Se phase. This multiphase system eventually results in the decline in the thermal conductivity of BA15SO as compared to that of BA20SO. The lowest thermal conductivity of 0.67 W/m.k was obtained for BA15SO at 773 K. However, the thermal conductivity for BA20SO was much increased with the increase of silver content, which may be remained unreacted in metallic form within the grains. The highest thermal conductivity was obtained at 473 K for BA20SO, which was almost 54 % higher than that of BA15SO at this temperature. Hence, it is concluded that the formation of such multi-phased system combined with nano-inclusion may be the potential candidate for thermoelectric applications.

References

1. Ruleova, P., et al., *Enhanced Thermoelectric Performance of n-type Bi2O2Se Ceramics Induced by Ge Doping.* Journal of Electronic Materials, 2018. **47**(2): p. 1459-1466.
2. Bell, L.E., *Cooling, Heating, Generating Power, and Recovering Waste Heat with Thermoelectric Systems.* Science, 2008.
3. Gorai, P., V. Stevanović, and E.S. Toberer, *Computationally guided discovery of thermoelectric materials.* Nature Reviews Materials, 2017. **2**(9): p. 17053.
4. Heremans, J.P., R.J. Cava, and N. Samarth, *Tetradymites as thermoelectrics and topological insulators.* Nature Reviews Materials, 2017. **2**(10): p. 17049.
5. Zeier, W.G., et al., *Engineering half-Heusler thermoelectric materials using Zintl chemistry.* Nature Reviews Materials, 2016. **1**(6): p. 16032.
6. Rhyee, J.-S., et al., *Peierls distortion as a route to high thermoelectric performance in In4Se3-δ crystals.* Nature, 2009. **459**(7249): p. 965-968.
7. Pei, Y., et al., *Convergence of electronic bands for high performance bulk thermoelectrics.* Nature, 2011. **473**(7345): p. 66-69.
8. Heremans, J.P., et al., *Enhancement of Thermoelectric Efficiency in PbTe by Distortion of the Electronic Density of States.* Science, 2008.

9. Poudel, B., et al., *High-Thermoelectric Performance of Nanostructured Bismuth Antimony Telluride Bulk Alloys.* Science, 2008.
10. Mao, J., et al., *High thermoelectric cooling performance of n-type Mg3Bi2-based materials.* Science, 2019.
11. Zhao, L.-D., et al., *Ultrahigh power factor and thermoelectric performance in hole-doped single-crystal SnSe.* Science, 2016. **351**(6269): p. 141-144.
12. Tan, X., et al., *Synergistical Enhancement of Thermoelectric Properties in n-Type Bi2O2Se by Carrier Engineering and Hierarchical Microstructure.* Advanced Energy Materials, 2019. **9**(31): p. 1900354.
13. Liu, R., et al., *Carrier concentration optimization for thermoelectric performance enhancement in n-type Bi2O2Se.* Journal of the European Ceramic Society, 2018. **38**(7): p. 2742-2746.
14. Wei, Q., et al., *Quasi-Two-Dimensional Se-Terminated Bismuth Oxychalcogenide (Bi2O2Se).* ACS Nano, 2019. **13**(11): p. 13439-13444.
15. Khan, U., et al., *Controlled Vapor–Solid Deposition of Millimeter-Size Single Crystal 2D Bi2O2Se for High-Performance Phototransistors.* Advanced Functional Materials, 2019. **29**(14): p. 1807979.
16. Tan, X., et al., *Enhanced thermoelectric performance of n-type Bi2O2Se by Cl-doping at Se site.* Journal of the American Ceramic Society, 2017. **100**(4): p. 1494-1501.
17. Yang, N., et al., *Effects of Sb-doping on the electron-phonon transport properties of Bi2O2Se.* Journal of Alloys and Compounds, 2021. **858**: p. 157748.
18. Kim, M., D. Park, and J. Kim, *Enhancement of Bi2O2Se thermoelectric power factor via Nb doping.* Journal of Alloys and Compounds, 2021. **851**: p. 156905.
19. Pan, L., et al., *Effects of sulfur substitution for oxygen on the thermoelectric properties of Bi2O2Se.* Journal of the European Ceramic Society, 2020. **40**(15): p. 5543-5548.
20. Zhan, B., et al., *Enhanced Thermoelectric Performance of Bi2O2Se with Ag Addition.* Materials, 2015. **8**(4): p. 1568–1576.
21. Voneshen, D.J., et al., *Suppression of thermal conductivity by rattling modes in thermoelectric sodium cobaltate.* Nature Materials, 2013. **12**(11): p. 1028-1032.
22. *Strategies for optimizing the thermoelectricity of PbTe alloys*. 2021.
23. Chen, J., et al., *Hierarchical Structures Advance Thermoelectric Properties of Porous n-type β-Ag2Se.* ACS Applied Materials & Interfaces, 2020. **12**(46): p. 51523-51529.
24. Ferrer-Argemi, L., et al., *Silver content dependent thermal conductivity and thermoelectric properties of electrodeposited antimony telluride thin films - Scientific Reports.* Scientific Reports, 2019. **9**(9242): p. 1-8.
25. Oluwalowo, A., et al., *Electrical and thermal conductivity improvement of carbon nanotube and silver composites.* Carbon, 2019. **146**: p. 224-231.